

UC Irvine

UC Irvine Previously Published Works

Title

Radiative forcing of natural forest disturbances

Permalink

<https://escholarship.org/uc/item/69n669bm>

Journal

Global Change Biology, 18(2)

ISSN

1354-1013

Authors

O'Halloran, Thomas L
Law, Beverly E
Goulden, Michael L
et al.

Publication Date

2012-02-01

DOI

10.1111/j.1365-2486.2011.02577.x

Supplemental Material

<https://escholarship.org/uc/item/69n669bm#supplemental>

Copyright Information

This work is made available under the terms of a Creative Commons Attribution License, available at <https://creativecommons.org/licenses/by/4.0/>

Peer reviewed

Radiative forcing of natural forest disturbances

THOMAS L. O'HALLORAN*, BEVERLY E. LAW*, MICHAEL L. GOULDEN†, ZHUOSEN WANG‡, JORDAN G. BARR§, CRYSTAL SCHAAF‡, MATHEW BROWN¶, JOSÉ D. FUENTES**, MATHIAS GÖCKEDE*, ANDREW BLACK¶ and VIC ENGEL§

*Department of Forest Ecosystems and Society, Oregon State University, Corvallis, OR 97331, USA, †Department of Earth System Science, University of California, Irvine, CA 92697, USA, ‡Center for Remote Sensing, Boston University, Boston, MA 02215, USA, §South Florida Natural Resource Center, Everglades National Park, Homestead, FL 33030, USA, ¶Faculty of Land and Food Systems, University of British Columbia, Vancouver, BC V6T 1Z4, Canada, **Department of Meteorology, Penn State University, University Park, PA 16802, USA

Abstract

Forest disturbances are major sources of carbon dioxide to the atmosphere, and therefore impact global climate. Biogeophysical attributes, such as surface albedo (reflectivity), further control the climate-regulating properties of forests. Using both tower-based and remotely sensed data sets, we show that natural disturbances from wildfire, beetle outbreaks, and hurricane wind throw can significantly alter surface albedo, and the associated radiative forcing either offsets or enhances the CO₂ forcing caused by reducing ecosystem carbon sequestration over multiple years. In the examined cases, the radiative forcing from albedo change is on the same order of magnitude as the CO₂ forcing. The net radiative forcing resulting from these two factors leads to a local heating effect in a hurricane-damaged mangrove forest in the subtropics, and a cooling effect following wildfire and mountain pine beetle attack in boreal forests with winter snow. Although natural forest disturbances currently represent less than half of gross forest cover loss, that area will probably increase in the future under climate change, making it imperative to represent these processes accurately in global climate models.

Keywords: albedo, beetles, carbon, disturbance, fire, forests, hurricane, radiative forcing

Received 24 August 2011; revised version received 24 August 2011 and accepted 15 September 2011

Introduction

Terrestrial disturbances are primary regulators of the global carbon cycle (Running, 2008), and can switch entire ecosystems from carbon sinks to sources (Luyssert *et al.*, 2008). Increasing evidence suggests major natural forest disturbances are increasing in frequency and/or intensity under climate change, including fire (Westerling *et al.*, 2006), insect outbreaks (Raffa *et al.*, 2008), and landfalling hurricanes (Bender *et al.*, 2010). Over the last decade, these three disturbances destroyed ca. 2–4 million ha of forest annually in the United States alone (Forest Service USDA, 2008; Schwind, 2008; Zeng *et al.*, 2009). In British Columbia (BC), the extent of forest mortality caused by mountain pine beetle (MPB) has reached unprecedented levels. In 2007, the affected area surpassed 10 million ha (Westfall & Ebata, 2009). A warming and drying in the region associated with climate change has allowed the beetle to expand its range to these exceptional limits (Carroll

et al., 2003). Warming climate has also contributed to increasing the size and frequency of wildfires (Kasischke & Turetsky, 2006). Over the last 50 years, an average 2 million ha of boreal forest have burned each year in North America (Stocks *et al.*, 2002). A recent estimate indicates that over the last 150 years, landfalling hurricanes have released an average 25 Tg of carbon per year in the United States alone (Zeng *et al.*, 2009). This is enough carbon to offset 9–18% of the annual US forest carbon sink. Hurricane Katrina destroyed an estimated 105 Tg of biomass when it made landfall on the US Gulf coast in 2005 (Chambers *et al.*, 2007).

However, little is known about the impacts of these forest disturbances on albedo, and therefore it is unclear whether these disturbances will generate reinforcing climate feedbacks (Dale *et al.*, 2001; Running, 2008; Adams *et al.*, 2010). Disturbances that decrease surface albedo (reflectivity) have the potential to create a positive (heating) radiative forcing by increasing the amount of solar radiation absorbed in the climate system. In the case of fire in boreal forests, the increase in surface albedo following fire can offset the heating associated with the carbon released to the atmosphere (Randerson *et al.*, 2006). This occurs under snowy conditions because open (i.e. burned) spaces, relative to

Correspondence: Thomas L. O'Halloran, Department of Environmental Studies, Sweet Briar College, Sweet Briar, VA 24595, USA, tel. +1 434 381 6389, fax +1 434 381 6494, e-mail: tohalloran@sbc.edu

forested space, create relatively homogenous snowy surfaces that have a very high albedo. Forests, in contrast, have structures such as foliage and branches that create and trap multiple reflections of incoming solar radiation and decrease albedo. The low albedo of boreal forests creates a relative radiative forcing equivalent to that provided by its sequestered carbon (Bonan *et al.*, 1992; Betts, 2000; Bala *et al.*, 2007; Bonan, 2008; Anderson *et al.*, 2011). Albedo effects can outweigh the climate benefits of carbon sequestration in boreal and semiarid forests, depending on integration time or duration of disturbance recovery (Betts, 2000; Rotenberg & Yakir, 2010).

Here, we quantify the radiative forcing associated with perturbations to atmospheric CO₂ (ΔF_{CO_2}) and surface albedo (ΔF_s) to weigh the climate effects (e.g. Betts, 2000; Randerson *et al.*, 2006; Rotenberg & Yakir, 2010) of major natural disturbance mechanisms from hurricane, wildfire and beetle attack.

Methods

We apply the concept of radiative forcing (Hansen *et al.*, 1997) to quantify the per-unit area climate impacts of forest disturbance from perturbations to surface albedo and the concomitant efflux of CO₂ associated with such disturbances in subsequent years. We define the net radiative forcing (ΔF_{net}) as the sum of two quantities: First, the shortwave radiative forcing (ΔF_s) is the mean annual change in reflected shortwave radiation at the top of the atmosphere resulting from changes in surface albedo. Second, radiative forcing caused by perturbations to atmospheric CO₂ from disturbance (ΔF_{CO_2}) was calculated from measured and modeled changes in net ecosystem carbon balance (NECB). For both quantities, the disturbed state is compared to the undisturbed state at an annual time step, and the net effect is determined over multiple years following several disturbance events. Instantaneous radiative forcings for albedo and CO₂ are evaluated in the absence of feedbacks, such as changes to cloudiness resulting from other potential biogeophysical impacts like perturbations to roughness or evapotranspiration. To define the impact of various types of disturbance on surface albedo, we analyzed both AmeriFlux micrometeorological tower observations (Law *et al.*, 2002) and MODIS broadband albedo (Schaaf *et al.*, 2002). Three case studies are presented, including (i) defoliation and mortality of a subtropical mangrove canopy by hurricane, (ii) forest mortality from MPB, and (iii) stand replacing fire in boreal forests.

Albedo radiative forcing

Albedo perturbation from forest disturbance was evaluated by comparing measurements of albedo in disturbed and undisturbed forests using both tower-based and remotely sensed datasets. Tower data were available for case studies of hurricane defoliation of a mangrove forest and wildfire in bor-

real forest. For those sites, daily values of albedo were calculated from tower-measured daily sums of half-hourly incoming and outgoing (reflected) shortwave radiation. Half-hourly values were excluded when the solar elevation angle (θ) did not exceed a minimum threshold (θ_{min}), which was set to approximately the local midday winter solstice value for each site, and therefore varied by latitude. Values of θ_{min} were 40° and 10° for the mangrove and boreal sites, respectively. The radiometer manufacturer (model CNR1 or CM3; Kipp & Zonen, Delft, the Netherlands) specifies an accuracy of 10% for daily sums of radiation. This corresponds to an uncertainty of ca. 0.015 in daily albedo measurements, and thus applies to all of our reported tower-measured albedo values.

Where tower data were not available, MODIS (MCD43A) broadband shortwave blue-sky albedo data (Schaaf *et al.*, 2002) were extracted using the MODIS subsetting tool (ORNL DAAC, 2011) for 6.25 km² areas (25 pixels) of interest for all available years (2000–2010). Only data that passed the quality control filters and were associated with the vegetation type of the center pixel were included. An aerosol optical depth of 0.2 was used in the calculation of blue-sky albedo. The accuracy of the MODIS Collection 5 shortwave albedo has been reported as 0.05 but is generally <0.03 (Roman *et al.*, 2009; Wang *et al.*, 2010). For each site, gaps in the 8 day MODIS albedo time series were filled by averaging values linearly interpolated across gaps with values taken from the 10 year ensemble average for that site, which has the benefit of constraining the local information provided by the interpolation with phenological and climatological information included in the ensemble average. This helps reduce interpolation errors from the discontinuities caused at the edges of snowy periods, where the albedo changes abruptly. The error associated with this technique was calculated by randomly creating and then filling a set of artificial gaps of the same length as the actual gaps. The bias error and root mean squared error were calculated by comparing the artificially filled and original time series. Results of 1000 simulations for each case (Table 1) show that the gap filling attributes negligible bias in all cases and only a significant root mean squared error in one case (boreal fire), where the large difference in summer and winter albedo make the gap filling more sensitive to error. Resulting potential errors in radiative forcing at the annual scale range from 0.05 to 0.59 W m⁻² and are incorporated in reported ranges of uncertainty. For the radiative forcing calculations, the 8 day MODIS values were averaged to monthly resolution.

The top-of-the-atmosphere (TOA) radiative forcing caused by the measured perturbations to surface albedo was calculated using the radiative kernel technique (Shell *et al.*, 2008; Soden *et al.*, 2008). The radiative kernel represents changes to TOA fluxes caused by incremental changes in monthly average surface albedo from present-day values at 2.5° resolution. It essentially represents a climatology of the sensitivity of TOA net shortwave radiation to incremental changes in albedo at the surface, neglecting feedbacks. The kernel used here was produced using the offline radiative transfer model of the National Center for Atmospheric Research (NCAR) Community Atmospheric Model version 3 (Collins *et al.*, 2006)

Table 1 Location, elevation, and statistics describing the error associated with gapfilling the MODIS time series of 8 day short-wave broadband albedo. Statistics include bias error (BE), root mean squared error (RMSE), and the average error imputed to the annual calculation of radiative forcing as calculated from the error statistics and 1000 Monte Carlo simulations

		Gapfilling error analysis						
		N gaps	BE	RMSE	RF error (std) (W m ⁻²)	Elevation (m)	Lat.	Lon.
Florida	Both	15	-9.73e-007 ± 4.94e-005	0.0011 ± 0.0002	0.05	0	25.39	81.13
Manitoba	Control	17	-6.14e-006 ± 1.74e-004	0.0036 ± 0.0012	0.1	250	56.37	-96.80
Manitoba	Fire	64	-1.75e-005 ± 9.59e-004	0.0191 ± 0.0035	0.59	200	56.36	96.37
Oregon	Control	86	-1.80e-005 ± 3.29e-004	0.0064 ± 0.0011	0.28	1600	44.00	-121.82
Oregon	Beetles	84	-8.48e-006 ± 4.64e-004	0.0093 ± 0.0019	0.41	1500	43.93	-121.76
BC	Control	16	-1.38e-005 ± 3.08e-004	0.0061 ± 0.0011	0.17	1300	53.08	-125.01
BC	Beetles	6	-1.06e-006 ± 2.42e-004	0.0053 ± 0.0014	0.16	900	53.19	-126.37

as described in (Shell *et al.*, 2008), but with an incremental albedo increase of 0.01 rather than 0.001. Relative to calculations of surface radiative forcing, using values of insolation measured at the surface, the TOA calculations with the kernel account for the attenuation of the upwelling beam by clouds and aerosols. It also accounts for spatial variability in incoming radiation. For example, annual average daily insolation measured at the surface was 18.4, 12.9, and 10.6 MJ m⁻² day⁻¹ for the Florida, Manitoba, and BC sites, respectively, presented in this study. The radiative forcing is then calculated at a monthly time step from perturbations in forest albedo caused by the disturbance relative to an undisturbed control stand. We report ranges of uncertainty in the radiative forcing that include 10% for accuracy in albedo measurements and an additional 10% associated with the radiative kernel technique.

CO₂ radiative forcing

To model the radiative forcing associated with the release of terrestrial carbon to the atmosphere due to disturbance, the concept of NECB was employed. NECB has been defined as the net carbon balance of an ecosystem, and includes net ecosystem exchange with the atmosphere (NEE) as well as lateral transport of carbon from disturbances and anthropogenic activities (Chapin *et al.*, 2006). Integrating NECB over larger spatial and temporal domains produces estimates of net biome productivity (NBP; Schulze & Heimann, 1998). Here, we are interested in the source of CO₂ to the atmosphere from changes to NECB (δNECB) resulting from a disturbance. δNECB represents the difference between the disturbed and undisturbed NECB, all else being equal, and is defined explicitly below for each of three case studies. The input of CO₂ to the global atmosphere in year t (δCO_{2t}) was calculated from annual δNECB_t using Eqn (1), where M_c is the molecular mass of carbon, M_a is the molecular mass of dry air, and m_a is the mass of the atmosphere.

$$\delta\text{CO}_{2t} = \frac{M_a \delta\text{NECB}_t}{M_c m_a} \quad (1)$$

The input of atmospheric CO₂ was drawn down in each year by terrestrial and ocean uptake by applying a response

function developed with the Bern 2.5 Carbon Cycle model (Joos *et al.*, 2001) and used in the IPCC radiative forcing calculations for atmospheric CO₂ (Forster *et al.*, 2007). Following uptake by biota and the oceans, the radiative forcing (ΔF_{CO_2}) associated with the resulting CO₂ perturbation (ΔCO_2) was calculated at an annual time step calculated using a well-known parameterization (Eqn 2; Myhre *et al.*, 1998), where CO₂* is the reference CO₂ concentration.

$$\text{RF} = 5.35 \times \ln \frac{\delta\text{CO}_2}{\text{CO}_2^*} \quad (2)$$

The reported radiative forcing represents that associated with the CO₂ perturbation from 1 m² of disturbed forest, mixed in the global atmosphere and then attributed to that 1 m², after uptake by the oceans and terrestrial biota. Therefore to convert the radiative forcings (both CO₂ and albedo) for comparison with global radiative forcings, they should be divided by the area of the earth. Ranges of uncertainty in ΔF_{CO_2} are calculated from the reported uncertainty in δNECB and an additional 10% associated with the radiative forcing parameterization (Myhre *et al.*, 1998). Where temporal trends are discussed, model statistics from least squares regression models are reported to indicate the statistical significance of those trends.

Hurricane defoliation of mangroves

Since 2004 an AmeriFlux micrometeorological tower (25°21' 46"N, 81°4'40"W) has operated near Shark River at the eastern edge of the Florida Everglades. Using the eddy covariance (EC) technique, the tower measures meteorological variables and determines turbulent heat and CO₂ fluxes (Barr *et al.*, 2010). The tower site is only 30 km from where the eye of hurricane Wilma made landfall on 24 October 2005. After achieving the lowest recorded central pressure of any hurricane in history, Wilma landed as a category 3 hurricane with sustained winds of 190 km h⁻¹ (Pasch *et al.*, 2006). The mangrove tower data record contains a 442 day gap associated with the destruction and eventual redeployment of the tower and instrumentation. As such, MODIS albedo was used to provide a continuous record both before and after the hurricane. Data from a 6.25 km² area adjacent to the tower site were extracted

for all available years (2000–2010) and the change in albedo caused by the hurricane was defined relative to monthly albedo values averaged over the prehurricane period (2000–2005).

Strictly speaking, NECB in this tidally driven mangrove forest is composed of temporal summations of net ecosystem exchange ($-\Sigma\text{NEE}$) and lateral fluxes of dissolved inorganic (DIC), dissolved organic (DOC), and particulate (PC) carbon entering or exiting the ecosystem (Chapin *et al.*, 2006). The δNECB is then:

$$\delta\text{NECB} = \Sigma\text{NEE}_{\text{disturbed}} + \Sigma\text{NEE}_{\text{undisturbed}} + \delta F_{\text{DIC}} + \delta F_{\text{DOC}} + \delta F_{\text{PC}},$$

where F represents lateral fluxes of carbon constituents with a positive sign convention for carbon entering the ecosystem. Fluxes of DIC, DOC, and PC (F_{DIC} , F_{DOC} , and F_{PC} , respectively), exported to the estuary may represent between 25% and 70% of $-\Sigma\text{NEE}$ based on regional and global estimates for mangroves while the remainder of $-\Sigma\text{NEE}$ is stored in biomass or soil carbon (Barr *et al.*, 2010). Although carbon leaves the flux footprint of the tower as DIC, DOC, and PC, some fraction is consumed or buried within the surrounding estuary and therefore remains sequestered. Without detailed estimates of lateral carbon fluxes, perturbations in these fluxes resulting from disturbance, and estimates of the amount of carbon remaining sequestered, our best estimate of δNECB excludes δF_{DIC} , δF_{DOC} , and δF_{PC} . The quantity $-\Sigma\text{NEE}_{\text{undisturbed}}$ ($1175 \pm 141 \text{ gC m}^{-2} \text{ yr}^{-1}$) was determined as the average of annual gap-filled NEE during 2004–2005 before the hurricane disturbance (Barr *et al.*, 2010). During the period following the hurricane in 2007–2010, $-\Sigma\text{NEE}_{\text{disturbed}}$ was the measured annual sum of $-\text{NEE}$ (Barr *et al.*, 2011). During 2006, EC estimates of NEE were only available during November and December, after the tower was rebuilt. For 2006 only, $-\Sigma\text{NEE}$ was determined as the difference between modeled gross primary production (GPP) and ecosystem respiration (R_{E}) rates. GPP 8 day estimates were determined from a vegetation photosynthesis model (Xiao *et al.*, 2004), which was trained using EC-derived GPP from the tower site from periods before (2004–2005) and after (2007–2009) hurricane disturbance. Drivers of modeled GPP (GPP_{mod}) included a green vegetation index derived from MODIS reflectance products as well as local climate data, including air temperature, photosynthetically active irradiance, and surface water salinity levels measured near the tower site. Monthly R_{E} was determined as the sum of expected respiration in an undisturbed mangrove forest (R_{Eundist}) and respiration contributed by the decomposition of coarse woody debris (R_{CWD}) resulting from tree mortality. Monthly R_{Eundist} was modeled using Eqn (2) with linear coefficients determined from least squares regression of monthly EC-derived GPP and R_{E} during 2004–2005.

$$R_{\text{Eundist}} = m\text{GPP}_{\text{mod}} + b. \quad (3)$$

Monthly R_{CWD} equaled the carbon content from the decomposition of dead trees. Cumulative tree mortality was measured at quarterly intervals in three circular plots adjacent to the tower (Smith *et al.*, 2009) starting November 2005. Decomposition rates of the coarse woody debris pool were assumed

to follow the exponential decay function of Romero *et al.* (2005). Their model includes rate constants for both labile and refractory biomass fractions of wood in three species of mangroves (*Rhizophora mangle* L., *Avicennia germinans*, and *Laguncularia racemosa*) on site. On an annual basis, modeled $-\Sigma\text{NEE}$ was 7–32% higher than EC-derived $-\Sigma\text{NEE}$ during 2007–2009. Modeled GPP was within 3% of EC-derived GPP estimates, suggesting an underestimate of R_{E} . Underestimates may have resulted from exclusion of root decomposition of the dead trees and increased soil respiration rates resulting from increased irradiance penetration to the surface and higher soil temperatures following hurricane disturbance (Barr *et al.*, 2011). To account for these and any other potential biases, the $-\Sigma\text{NEE}$ estimate for 2006 was taken as the average of bias-corrected $-\Sigma\text{NEE}$ estimates (average of $-\Sigma\text{NEE}_{2006}/1.07$ and $-\Sigma\text{NEE}_{2006}/1.32$). Given that model uncertainties in $-\Sigma\text{NEE}$ for 2006 were expected to be larger than those during years when $-\Sigma\text{NEE}$ was determined from EC data, an additional constraint was applied to $-\Sigma\text{NEE}$ during the first full year of recovery in 2006. The $-\Sigma\text{NEE}$ (\pm uncertainty) during 2007 and subsequent years of recovery should equal or exceed the $-\Sigma\text{NEE}$ estimate for 2006. This constraint was based on both higher R_{E} and lower or equal GPP rates during the first full year of recovery compared to those rates in subsequent years. Mortality rates of mature trees reached 20% before 2007 and reached a maximum of 30% by mid-year 2009 (Barr *et al.*, 2011). Based on the exponential decay function of Romero *et al.* (2005), R_{CWD} , and therefore its contribution to R_{E} , would have been highest during November 2005–December 2006 when the pool of labile biomass of dead wood was at a maximum. Model estimates of GPP were also lower during the first half of 2006 as a result of reduced green vegetation cover compared to later periods.

Mountain pine beetle

Mountain pine beetle has impacted millions of hectares of pine forests in western North America in the last decade (Raffa *et al.*, 2008). In BC, the outbreak has reached epidemic proportions (Kurz *et al.*, 2008), with significant infestations also extending southward into the United States along the Cascade and Rocky Mountain ranges into Washington, Oregon, Idaho, Montana, Wyoming, and Colorado. Here, we develop two case studies to quantify the impact of mortality in lodgepole pine stands from MPB infestation in BC and Oregon. In BC, some of the earliest beetle infestations of the recent epidemic occurred in Northern Tweedsmuir and Entiako Provincial Parks starting in 1994 (Garbutt, 1994). Aerial surveys in 1999 (Cichowski *et al.*, 2001) revealed the attack in those areas was severe (30–100% infestation) with some areas already experiencing dead, or gray-attacked trees. Using a combination of those surveys and contemporary LANDSAT imagery we have identified four beetle-attacked stands in that region that have not burned or been salvaged as of 2010 (Table 1). To isolate the beetle effect on albedo from interannual variability in snow pack, a nearby control stand was identified with little or no beetle attack. Due to the ubiquity of attack in mature lodgepole stands in the region, the unattacked stand necessarily

contains a significant proportion of subalpine fir and spruce in addition to lodgepole pine, and occurs at slightly higher elevation (1300 vs. 1000 m). MODIS blue-sky broadband albedo data were extracted for 6.25 km² areas for each of the four beetle-attacked sites and the control site. To improve statistics, the time series of albedo at the four attacked sites were averaged together and an average year of attack of 1996 was assumed.

As a replicate of the albedo analysis in BC we also identified an MPB-attacked stand in Oregon, ca. 1000 km south of the BC sites. US Forest Service aerial survey data (Forest Service USDA, 2010) were used to identify a beetle infested lodgepole pine stand in the central Oregon Cascades where red attack was first detected in 1996. MODIS blue-sky albedo data were extracted for an attacked and adjacent control site (Table 1), from which the albedo perturbation from beetles was defined.

The effect of beetle mortality on productivity in lodgepole pine forests of BC has been reported by Kurz *et al.* (2008). For the current outbreak, they report NBP from 2000 to 2006 based on forest inventory data, and develop model projections for 2007–2020. A baseline control NBP was reported that incorporated regional rates of harvest and fire in the absence of beetles, and a beetle case included the additional effect of beetle, but not additional harvest (Kurz *et al.*, 2008). Here, we define the net effect of the beetles (δNECB) as the difference between the reported NBP values for the beetle and control cases, to remove the effects of harvest and fire. Mean annual δNECB began at $-0.7 \pm 2 \text{ gC m}^{-2} \text{ yr}^{-1}$ in the first year and increased to a max of $-54 \pm 22 \text{ gC m}^{-2} \text{ yr}^{-1}$ at 10 years since attack. Mean annual δNECB over the first 14 years was $-33 \pm 16 \text{ gC m}^{-2} \text{ yr}^{-1}$.

Boreal fire

A mesonet of six tower sites in Manitoba, Canada, that represent a chronosequence of coniferous forest sites with mean stand ages ranging from 11 to 159 years since fire, provided measurements of radiation, heat, and carbon dioxide fluxes between 2001 and 2005 (Amiro *et al.*, 2006; Goulden *et al.*, 2006; Mcmillan & Goulden, 2008). The sites, which range in vegetation cover from early successional herbs to mid-aged jack pine and mature black spruce, experience similar climate and have similar soil types and drainages (Goulden *et al.*, 2006), providing an unprecedented opportunity to study carbon and energy cycling in the boreal forests, including patterns of albedo after fire (Amiro *et al.*, 2006; Goulden *et al.*, 2006; Mcmillan & Goulden, 2008). Here, we extend beyond previous albedo analyses by averaging all the available data from 2001 to 2005 to produce monthly, seasonal, and annual site means of albedo. To fill the albedo record in the first 10 years following fire, we extracted MODIS albedo for a burn that occurred in 1998 and an adjacent control stand in the same ecoregion as the mesonet, 100 km to its northeast (Table 1). The fire was identified using the Canadian Large Fire Database (Stocks *et al.*, 2002). Seasonal and annual means of albedo from MODIS and the tower chronosequence were combined and fit with exponential functions to provide continuous estimates of boreal albedo for years 2–159 after fire.

The agreement between the tower and MODIS data is excellent, which is consistent with a formal evaluation that included these sites (Wang *et al.*, 2010). The radiative forcing was calculated from albedo perturbations relative to the MODIS control stand for the MODIS data, and from the oldest site in the chronosequence (159 years) for the other tower sites. To produce continuous values of ΔF_{sw} , the combined time series of annual radiative forcing was modeled with a two-term exponential function ($R^2 = 0.90$, $P < 0.001$).

Biometric and EC measurements of carbon stocks and fluxes were also measured at the tower mesonet (Goulden *et al.*, 2011). For those sites δNECB was defined as $\delta\text{NECB} = \text{NECB}_{\text{disturbed}} - \text{NECB}_{\text{undisturbed}}$, where $\text{NECB}_{\text{disturbed}}$ was determined from net ecosystem production (NEP) in the first 100 years following fire, but includes the pyrogenic flux in year 1. That is, in year 1 $\text{NECB}_{\text{disturbed}} = \text{NEP} - \text{Ld}$, where Ld is the pyrogenic flux due to the combustion of forest biomass. NEP was measured using the EC technique (Goulden *et al.*, 2011). Annual NEP data for the seven sites were fit with a four-parameter lognormal function that was used to model NEP at an annual time step (Fig. 1). To be consistent with an average fire return interval of ca. 80 years in this region (Harden *et al.*, 2000; Manies *et al.*, 2005), pyrogenic carbon emissions were calculated for the 74 year stand by applying combustion factors (Campbell *et al.*, 2007) to measurements of four carbon pools, including live vascular, live moss, forest floor (dead moss, leaf litter, fine debris and partially decomposed organic material above the mineral soil), and coarse woody debris (Goulden *et al.*, 2011). The resulting estimate is a pyrogenic flux of $1720 \pm 370 \text{ gC m}^{-2}$ from the fire at time zero, where the range is based on the uncertainty in both the carbon stock measurements and the emission factors. This falls within the range of $1235 \pm 410 \text{ gC m}^{-2}$ reported as the 1959–1999 average for this ecoregion (Amiro *et al.*, 2001) and estimates from other northern coniferous forests of 1900 ± 250 and 1246 gC m^{-2} (Randerson *et al.*, 2006; Campbell *et al.*, 2007), respectively. Given a mean stand age of 74 years at the

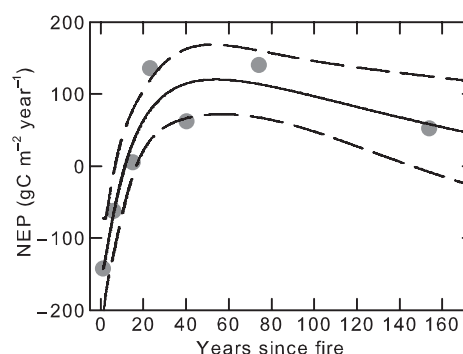


Fig. 1 Mean annual net ecosystem production (NEP) as measured with eddy covariance across the boreal chronosequence (Goulden *et al.*, 2011) with 25th and 75th percentile confidence intervals of a four-parameter lognormal fit ($R^2 = 0.88$, $P < 0.07$). The model fit is used to predict NEP at an annual time scale. The ecosystem is a carbon source for approximately the first 11 years following fire.

time of fire, $NECB_{undisturbed}$ was estimated as NEP from years 74 to 174 from the extrapolated model fit to measured NEP.

Results

Case studies

Hurricane defoliation of mangroves. In the Florida Everglades, Hurricane Wilma partially defoliated at least 270 000 ha of coastal mangrove forest. MODIS imagery indicates a reduction in the enhanced vegetation index (EVI), an indicator of canopy light interception, of as much as 80% in some areas (Fig. 2). Removal of the mangrove foliage and damage to the canopy exposed the dark, moist underlying surface (Fig. 3), resulting in a reduction in mean annual albedo from 0.11 to 0.09 in the year after the hurricane (Fig. 4). Due to high levels of insolation, this translates to $\Delta F_{\alpha} = 3.6 \pm 0.5 \text{ W m}^{-2}$ in the first year (Fig. 5a). Albedo recovered toward prehurricane values in the first 3 years following Hurricane Wilma, and has remained unchanged during the last 2 years. The reduction in albedo remains statistically significant 5 years following the hurricane (Student's *t*-test, $P < 0.001$). At the same time, the damage to the canopy also caused a large reduction in gross photosynthesis (GPP) and an increase in ecosystem respiration (Barr *et al.*, 2011). In the first 5 years following the hurricane, the average $\delta NECB$ was $-344 \pm 54 \text{ gC m}^{-2} \text{ yr}^{-1}$. As CO_2 emission from the disturbance accumulates in the atmosphere, the radiative forcing associated with $\delta NECB$ (ΔF_{CO_2}) increases. Over the 5 years following the hurricane the sum of the two positive (heating)

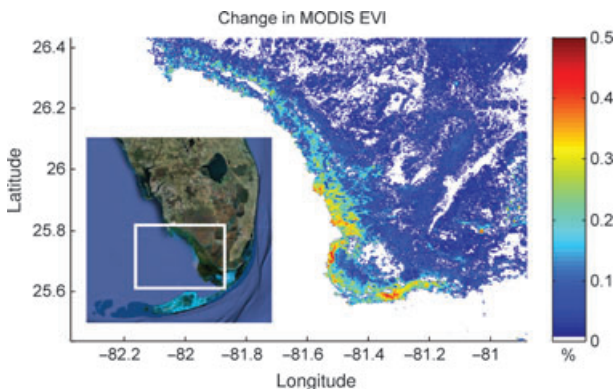


Fig. 2 Difference in MODIS enhanced vegetation index (EVI) from before and after hurricane Wilma, expressed as percent change. Three 16 day EVI scenes from November and December were averaged before Wilma in 2004 and after in 2005 to produce the difference. The inset shows southern Florida with the area of EVI analysis indicated by a white box. Visible imagery used in fair use, ©2011 Google, imagery © 2011 Terra-Metrics.

forcings results in an average net radiative forcing of $5.3 \pm 1.0 \text{ W m}^{-2}$ that is still increasing with time (Fig. 5a), where the albedo forcing accounted for 45% of the total forcing.

Mountain pine beetle. Mortality in forests attacked by insects was thought to have only a small effect on albedo (Running, 2008). Here, we find that that defoliation caused by the beetles only marginally affects summer albedo, but significantly increases winter albedo. In both BC and Oregon, the winter albedo had already increased by 0.06 at 4 years following attack (Fig. 6), suggesting that the dead trees had already shed their needles, exposing the underlying snow. Winter albedo in coniferous forests experiencing snow is particularly sensitive to the degree of canopy cover, because less foliage exposes underlying snow and increases albedo (Amiro *et al.*, 2006; Mcmillan & Goulden, 2008). In BC, the winter albedo perturbation then decreased until 9 years after attack, before increasing to another local maximum of 0.08 at 11 years. The albedo perturbation in Oregon followed the same general pattern, such that the winter values at both sites could be described by a periodic Fourier function (Fig. 6; $R^2 = 0.76$, $P < 0.001$). The resulting radiative forcing at the BC site (Fig. 5b) started at $-1.9 \pm 0.3 \text{ W m}^{-2}$ at year 4 and then oscillated, reaching a local minimum at 8 years, with another local maximum of $-2.4 \pm 0.4 \text{ W m}^{-2}$ at year 11. The radiative forcing in years 1–3 was assumed to decrease linearly to zero at time zero.

The average CO_2 radiative forcing associated with ($\delta NECB$) averaged over the 14 year study period was $0.49 \pm 0.15 \text{ W m}^{-2}$ for the MPB study (Fig. 5b). Thus, the magnitude of ΔF_{α} exceeded ΔF_{CO_2} and opposed it in sign over the 14 year period, and the resulting mean net forcing was $-0.98 \pm 0.3 \text{ W m}^{-2}$ (cooling effect).

Boreal fire. For the wildfire cases, results of the MODIS analysis show that albedo was initially elevated (compared to mature stands) in all seasons 2 years after fire, and then further increased with time for the next 10 years (Fig. 7). Tower data from the mesonet agree well with MODIS data for the year of overlap (year 11) and then indicate an exponential decay of albedo in all seasons toward mature boreal values over the next 100 years (Mcmillan & Goulden, 2008). Model fits to the data shown in Fig. 7 are provided in an Appendix S1. This results in an annual radiative forcing that increases until ca. 10–20 years following fire, and then decreases exponentially with time (Fig. 5c). In the first 20 years following fire, NEP and $\delta NECB$ were negative (Fig. 1), creating a large relative source of CO_2 to the atmosphere. The resulting radiative forcing, ΔF_{CO_2} , peaked at year 10 (Fig. 5c) and then decreased to

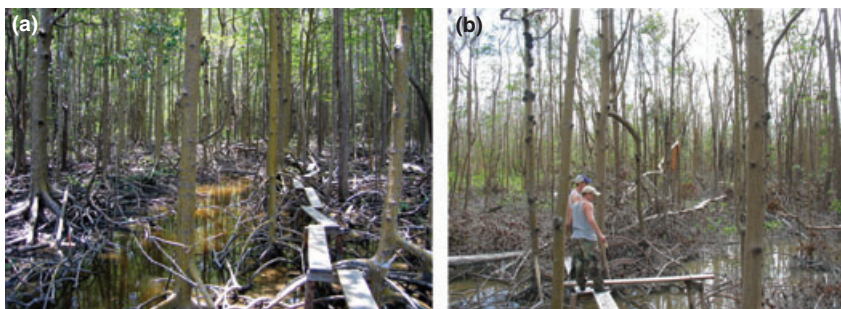


Fig. 3 (a) View of the understory and boardwalk leading to the tower at the mangrove site before the hurricane shows a closed canopy. (b) After the hurricane the canopy was nearly completely removed, exposing the dark, damp soil.

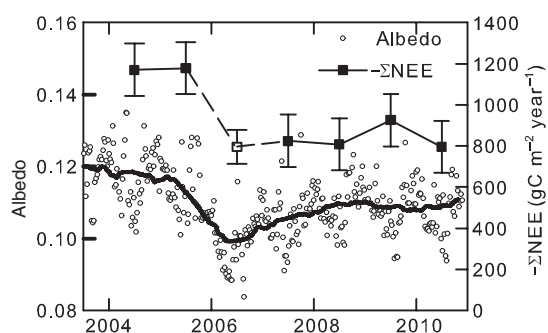


Fig. 4 Time series of MODIS 8 day shortwave broadband albedo (hollow circles) with annual moving average (solid line, left axis), and annual tower-measured and modeled $-\Sigma\text{NEE}$ with uncertainty estimates (squares with error bars, right axis). The value of $-\Sigma\text{NEE}$ in 2006 is shown as a hollow square to indicate that the value was modeled rather than measured, as in other years. The impact of defoliation from Hurricane Wilma is visible as a significant reduction in both albedo and $-\Sigma\text{NEE}$.

become negative following year 65. This occurs because δNECB remains positive while NEP in the mid-successional stage exceeds that of late successional undis-

turbed stands (Luyseart *et al.*, 2008). Subsequently, large opposing values of ΔF_{CO_2} and ΔF_{α} mostly balanced in the first 50 years, with ΔF_{CO_2} dominating in the first 10 years due to the initial large pyrogenic pulse of CO_2 . The average ΔF_{net} over the first 50 years was $0.59 \pm 3.8 \text{ W m}^{-2}$ (warming effect) and $-2.4 \pm 1.0 \text{ W m}^{-2}$ (cooling effect) in the next 50 years. The average net radiative forcing over 100 years was $-0.9 \pm 2.4 \text{ W m}^{-2}$.

Discussion

In each of our case studies, the albedo change associated with a stand-altering forest disturbance caused a radiative forcing on the same order of magnitude as the concomitant CO_2 forcing. The mangrove/hurricane case provided the only example in which the CO_2 and albedo forcings were both positive, resulting in a large net heating. With both beetle attack and fire, where snow is present, the removal of the canopy greatly increases albedo, creating a cooling radiative forcing relative to the CO_2 forcing. We hypothesize that the albedo radiative forcing (whether positive or negative)

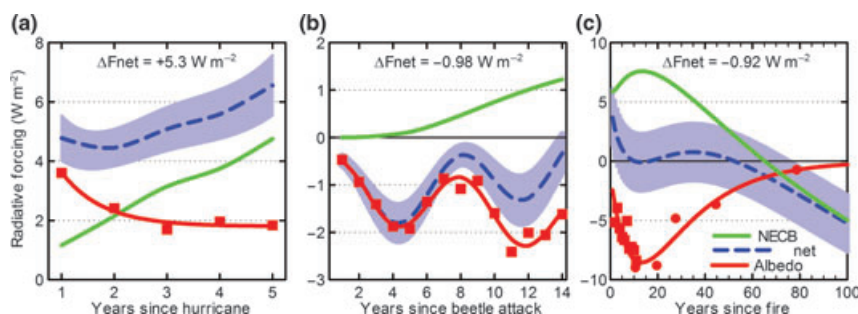


Fig. 5 Top of the atmosphere radiative forcing resulting from changes to albedo (data as red symbols; model fit as red line) and net ecosystem production (δNECB , green line) and the net of those two processes (dashed blue line) for (a) hurricane damage to a mangrove forest, (b) lodgepole pine mortality from mountain pine beetle, (c) stand replacing fire in coniferous forests in and Manitoba, Canada (squares = MODIS; circles = towers). Values of ΔF_{net} averaged over the period indicated in each panel are included. The radiative forcing from albedo changes and CO_2 release are on the same order of magnitude, and can either oppose in sign to reduce the net forcing (e.g., b, c), or combine constructively to enhance it (e.g., a).

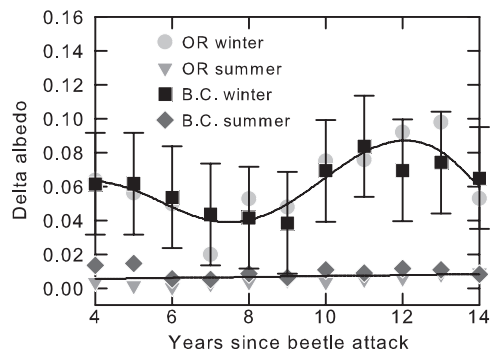


Fig. 6 Time series of the perturbation of MODIS albedo in summer (JJAS) and winter (NDJF), as a function of years since mountain pine beetle attack in lodgepole pine stands in British Columbia (BC) and Oregon (OR). Albedo is greatly enhanced in winter after the dead trees drop their needles. The albedo perturbation changes with time as the degree of canopy openness is controlled by the balance of the release of surviving trees and fall of standing dead branches and snags. Error bars are shown on the BC winter values to indicate the reported accuracy of MODIS albedo data.

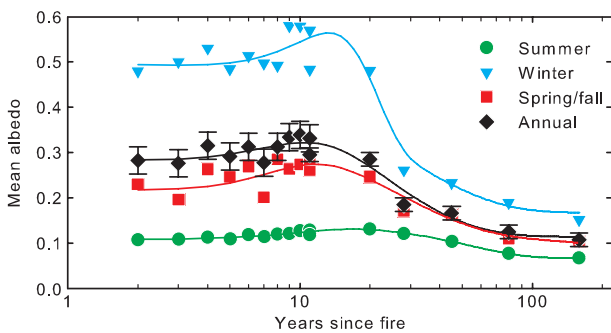


Fig. 7 Annual and seasonally averaged albedo as a function of years since fire (stand age) for summer (JJAS), winter (JFMD), and spring/fall (AMON). Data from years 2 to 11 since fire are MODIS data, and years 11–159 are tower data from the boreal chronosequence. Model fits are two-term exponential functions (see Supporting Information). Error bars on the annual albedo means indicate confidence intervals of 0.03 for MODIS data and 0.015 for tower data.

will be significant relative to the CO_2 radiative forcing in most stand-altering forest disturbances, as the albedo of underlying soil or early successional species (e.g. grasses) is rarely the same as the forest albedo. This is especially important in high latitude or elevation sites that experience snow because of the well-documented snow-masking effect of forests (Mcfadden & Ragotzki, 1967; Betts & Ball, 1997). Furthermore, in colder environments, where succession tends to proceed slower, the recovery to predisturbance albedo is slower, extending the longevity of the radiative forcing. In our boreal fire example, the albedo radiative forcing

persisted for ca. 100 years, while in contrast, the subtropical mangrove forest recovered half of its albedo perturbation in only 2 years. At the time of writing, at 5 years since hurricane, both albedo and $-\Sigma\text{NEE}$ are still suppressed in the mangroves, such that the radiative forcing is still nonzero. The duration of those forcings can only be determined by continuing to monitor these processes into the future.

The decrease in albedo in the mangroves may be relatively unique, as even in other tropical environments, albedo tends to increase following deforestation because of the quick establishment of grasses, which have a higher albedo than forest. Evidence from the tropics suggests that following clearing, pasture albedo, when left to return to forest, can return to predisturbance tropical forest values in ca. 30 years (Giambelluca, 2002), well before the carbon stocks. These examples also highlight the complexity in determining the net climate effect of forest disturbances, as the albedo and carbon components can recover at different rates. This occurs because the radiative properties of the canopy (i.e., albedo) depend on canopy geometry, which may have controls in addition to the ecological controls governing succession and recovery of carbon stocks (e.g. competition for light, water, and nutrients). In mangroves, the quick, but partial recovery of albedo was not matched by recovery in $-\Sigma\text{NEE}$. This is likely related to the early recovery of foliage and growth of epicormic sprouts, which partially close the canopy and affect albedo. However, leaf area index and density of photosynthetically active vegetation has likely not been restored to predisturbance conditions as evidenced by reduced EVI in the 2.5 by 2.5 km grid centered on the tower site (Barr *et al.*, 2011). In addition, higher respiratory fluxes have persisted during the 5 years following the storm as the result of several factors including decomposition of storm-generated coarse woody debris, statically unstable conditions which characterized the canopy air mass, and higher post-storm soil temperatures, especially during dry seasons when water levels are seasonally low.

The beetle case illustrates another level of complexity, where the disturbance is not as discrete or as complete as other disturbances, such as severe fire. This results in a disturbance in albedo and carbon stocks that amplifies for some time before transitioning into recovery. The net effect to carbon stocks (and albedo, we hypothesize) depends on the death, decay, and fall of trees over several years, balanced with the release of understory and surviving trees made possible by the increasing availability of resources, such as light (Waring & Pitman, 1985). Estimates of NEP show that the loss of productivity from dead trees may be balanced by the release of surviving trees in the first few years

following attack (Brown *et al.*, 2010). MPB-killed trees lose nearly all their needles by 4 years after attack (Safarynik *et al.*, 2006). We find that this significantly increases winter (and annual) albedo. Following that, albedo actually decreased for a few years. We hypothesize that this may reflect the initial release of surviving and understory trees. After about 9 years, albedo began to increase again, perhaps as fine branches, and the smallest snags began to fall. This is again followed by a decrease in albedo. We hypothesize that this may be followed by one final increase in albedo that would be associated with the fall of the remaining larger snags, which could open the canopy to its barest state. In Oregon, MPB-killed lodgepole pine trees in unthinned forests were found to begin to fall 5 years following death (Mitchell & Preisler, 1998), where 50% were down by 9 years, and 90% by 14 years. Significant blowdown has not yet been observed in our study areas around Eutsuk Lake, and is expected to occur soon, in years 15–20 following attack (D. Coates, personal communication). Albedo radiative forcing will likely reach peak negative values at that time. MPB-killed lodgepole tend to break and fall from the base (Mitchell & Preisler, 1998), so that the process is partially controlled by the decay rate at the base, which will be a function of moisture and temperature, among other variables. The other major control of snag fall rate is the experienced wind speed, which for any given snag can be a function of local weather and climatology, elevation, aspect, stand density, etc. This may lead to a large degree of variability in the timing of snag fall, and our case study should be viewed as one example. Continued measurements and monitoring will be required to determine the duration and net impact of the beetle epidemic. At the landscape scale, the most important control on the albedo perturbation is likely the severity of attack, which varies from just a few attacked trees, to near complete stand replacement. This is also the most important predictor of the impact to carbon stocks, where recovery relative to unattacked stands can take decades. Measurements and simulations from MPB-attacked lodgepole stands from the current epidemic in Idaho indicate recovery of attacked carbon stocks can take anywhere from 56 to 185 years, depending mostly on the severity of attack (Pfeifer *et al.*, 2011).

Our postboreal fire analysis supports previous findings that summer albedo tends to increase with time starting 2 years after fire as early successional herbs, shrubs, and deciduous seedlings begin to reestablish (Amiro *et al.*, 2006; Randerson *et al.*, 2006; Lyons *et al.*, 2008; Mcmillan & Goulden, 2008). The greatest increase in albedo occurs in winter (Liu *et al.*, 2005; Amiro *et al.*, 2006; Randerson *et al.*, 2006; Liu & Randerson, 2008), where the loss of canopy creates a much more reflective

surface for lying snow (Betts & Ball, 1997). This mechanism also increases albedo in spring and fall (Liu *et al.*, 2005; Randerson *et al.*, 2006; Lyons *et al.*, 2008) which represent the transition period for snow cover, making albedo during these times especially sensitive to inter-annual variability in snowfall (Liu *et al.*, 2005). In our analysis, winter albedo increased with time in the first 10 years following fire. As with the beetle case, we hypothesize that this increase in time may result from the fall of standing dead snags. The time it takes for half of dead snags to fall (i.e. half life) has been reported as 5–15 years after fire in smaller fire-killed coniferous trees in western North America (Russell *et al.*, 2006). Thus, the progression of seasonal albedo with time during recovery not only depends on the rate of reestablishment during succession, but also the loss of standing dead snags and branches following fire.

Addressing multiple disturbances across very different biomes necessitated employing a variety of measurement and modeling techniques within this work. We have attempted to quantify and highlight the uncertainties in these techniques throughout. To the best of our knowledge, no systematic biases have been imputed from the diversity of methodologies. The greatest shortcoming of this work may be the duration of beetle and hurricane cases studies, which do not capture the full recovery of the ecosystems to pre-disturbance levels of albedo or NECB. Continued measurement and monitoring will be required of ongoing work to determine the duration and net climate impact of these disturbances.

Conclusions

This analysis shows that, in terms of radiative forcing, albedo perturbations from natural forest disturbances can impact climate as much as the associated relative source of CO₂ to the atmosphere. Depending on the disturbance, the net of these two forcings can be positive (heating) or negative (cooling) when averaged over the measurement period. That is, the albedo effect can either enhance or reduce the positive radiative forcing from CO₂ efflux, depending on the albedo of the underlying soil and early successional vegetation type, as well as the climate zone. Defining the net impact of a disturbance requires integration of fluxes and albedo over long timeframes, on the order of 100 years. Generally, in places that experience snow, removal of forest canopy via disturbance will lead to an increase in albedo. The magnitude of that increase depends on the severity of disturbance, pre-existing stand density, snow amount, and radiation environment (e.g., latitude). However, albedo can also decrease after a disturbance, as demonstrated by our hurricane-defoliated

mangrove case. The rate of recovery of albedo depends on the complex controls governing the ecological processes of succession, which also determine the recovery of carbon stocks. However, albedo and carbon stocks are not exactly coupled during succession, highlighting the complexity of representing these processes in global climate models. These processes vary greatly across ecoregions, and representing them properly will require continued use of carbon flux measurements, biometry, and remote sensing. Improving our understanding of these processes is particularly crucial with regard to global scale prognostic climate modeling, since natural disturbances are expected to increase under a changing climate. This study adds to a now considerable body of work suggesting that albedo needs to be incorporated into carbon/climate management decisions.

Acknowledgements

This research was supported by AmeriFlux [the Office of Science (BER), US Department of Energy (DOE; DE-FG02-04ER63917 and DE-FG02-04ER63911)]. Thanks to Robert Kennedy and Travis Woolley for help identifying fires and beetle disturbances in Oregon, Tara Hudiburg for inventory data analysis, Werner Kurz and Graham Stinson for Canadian NBP data, and John Campbell, Jeff Masek, Feng Gao, and Andres Schmidt for helpful discussions. Thanks to Deborah Cichowski, Arthur Stock, Cathy Middleton, and Tim Ebata for help identifying beetle disturbances in BC, and to Virginia Butner and Becky Bonney for editorial help.

References

- Adams HD, Macalady AK, Breshears DD *et al.* (2010) Climate-induced tree mortality: earth system consequences. *EOS Transactions*, **91**, 153–154.
- Amiro BD, Todd JB, Wotton BM *et al.* (2001) Direct carbon emissions from Canadian forest fires, 1959–1999. *Canadian Journal of Forest Research-Revue Canadienne De Recherche Forestiere*, **31**, 512–525.
- Amiro BD, Orchansky AL, Barr AG *et al.* (2006) The effect of post-fire stand age on the boreal forest energy balance. *Agricultural and Forest Meteorology*, **140**, 41–50.
- Anderson RG, Canadell JG, Randerson JT *et al.* (2011) Biophysical considerations in forestry for climate protection. *Frontiers in Ecology and the Environment*, **9**, 174–182.
- Bala G, Caldeira K, Wickett M, Phillips TJ, Lobell DB, Delire C, Mirin A (2007) Combined climate and carbon-cycle effects of large-scale deforestation. *Proceedings of the National Academy of Sciences of the United States of America*, **104**, 6550–6555.
- Barr JG, Engel V, Fuentes JD, Zieman JC, O'Halloran TL, Smith TJ, Anderson GH (2010) Controls on mangrove forest-atmosphere carbon dioxide exchanges in western Everglades National Park. *Journal of Geophysical Research-Biogeosciences*, **115**, doi: 10.1029/2009JG001186.
- Barr JG, Engel V, Smith TJ, Fuentes JD (2011) Hurricane disturbance and recovery of energy balance, CO₂ fluxes and canopy structure in a mangrove forest of the Florida Everglades. *Agricultural and Forest Meteorology*, doi: 10.1016/j.agrformet.2011.07.022.
- Bender MA, Knutson TR, Tuleya RE, Sirutis JJ, Vecchi GA, Garner ST, Held IM (2010) Modeled impact of anthropogenic warming on the frequency of intense Atlantic hurricanes. *Science*, **327**, 454–458.
- Betts RA (2000) Offset of the potential carbon sink from boreal forestation by decreases in surface albedo. *Nature*, **408**, 187–190.
- Betts AK, Ball JH (1997) Albedo over the boreal forest. *Journal of Geophysical Research-Atmospheres*, **102**, 28901–28909.
- Bonan GB (2008) Forests and climate change: forcings, feedbacks, and the climate benefits of forests. *Science*, **320**, 1444–1449.
- Bonan GB, Pollard D, Thompson SL (1992) Effects of boreal forest vegetation on global climate. *Nature*, **359**, 716–718.
- Brown M, Black TA, Nestic Z *et al.* (2010) Impact of mountain pine beetle on the net ecosystem production of lodgepole pine stands in British Columbia. *Agricultural and Forest Meteorology*, **150**, 254–264.
- Campbell J, Donato D, Azuma D, Law B (2007) Pyrogenic carbon emission from a large wildfire in Oregon, United States. *Journal of Geophysical Research-Biogeosciences*, **112**, doi: 10.1029/2007JG000451.
- Carroll AL, Taylor SW, Régnière J, Safranyik L (2003) *Effects of Climate Change on Range Expansion by the Mountain Pine Beetle in British Columbia*. Mountain Pine Beetle Symposium: Challenges and Solutions, October 30–31, 2003, Kelowna, British Columbia (eds Shore TL, Brooks JE, Stone JE), pp. 223–232. Natural Resources Canada. Canadian Forest Service, Pacific Forestry Centre, Information Report BC-X-399, Victoria, BC.
- Chambers JQ, Fisher JI, Zeng H, Chapman EL, Baker DB, Hurtt GC (2007) Hurricane Katrina's Carbon Footprint on U.S. Gulf Coast Forests. *Science*, **318**, 1107.
- Chapin FS, Woodwell GM, Randerson JT *et al.* (2006) Reconciling carbon-cycle concepts, terminology, and methods. *Ecosystems*, **9**, 1041–1050.
- Cichowski D, Lawson B, Williston P *et al.* (2001) *North Tweedsmuir Provincial Park Strategic Vegetation Management Study*. Prepared for BC Parks, Smithers, BC.
- Collins WD, Bitz CM, Blackmon ML *et al.* (2006) The Community Climate System Model version 3 (CCSM3). *Journal of Climate*, **19**, 2122–2143.
- Dale VH, Joyce LA, McNulty S *et al.* (2001) Climate change and forest disturbances. *BioScience*, **51**, 723–733.
- Forest Service USDA (2008) Major Forest Insect and Disease Conditions in the United States: 2008 Update. Forest Service USDA, Washington, DC.
- Forest Service USDA (2010) Forest Health Protection (FHP) Aerial Survey Data and Maps. Forest Service USDA, Washington, DC.
- Forster P, Ramaswamy V, Artaxo P *et al.* (2007). Changes in atmospheric constituents and in radiative forcing. In: *Climate Change 2007: The Physical Science Basis (Contribution of Working Group I to the Fourth Assessment Report of the Intergovernmental Panel on Climate Change)* (eds Nakajima T, Ramanathan V), pp. 129–234. Cambridge University Press, New York, NY, USA.
- Garbutt R (1994) *Mountain pine beetle and Western Balsam Bark Beetle in Tweedsmuir Provincial Park Prince Rupert Forest region*. FIDS Pest Report 94-13, Canadian Forest Service, Victoria, BC.
- Giambelluca TW (2002) Hydrology of altered tropical forest. *Hydrological Processes*, **16**, 1665–1669.
- Goulden ML, Winston GC, Mcmillan AMS, Litvak ME, Read EL, Rocha AV, Elliot JR (2006) An eddy covariance mesonet to measure the effect of forest age on land-atmosphere exchange. *Global Change Biology*, **12**, 1–17.
- Goulden ML, Mcmillan AMS, Winston GC, Rocha AV, Manies KL, Harden JW, Bond-Lamberty BP (2011) Patterns of NPP, GPP, respiration, and NEP during boreal forest succession. *Global Change Biology*, **17**, 855–871.
- Hansen J, Sato M, Ruedy R (1997) Radiative forcing and climate response. *Journal of Geophysical Research-Atmospheres*, **102**, 6831–6864.
- Harden JW, Trumbore SE, Stocks BJ, Hirsch A, Gower ST, O'Neill KP, Kasischke ES (2000) The role of fire in the boreal carbon budget. *Global Change Biology*, **6**, 174–184.
- Joos F, Prentice IC, Sitch S *et al.* (2001) Global warming feedbacks on terrestrial carbon uptake under the Intergovernmental Panel on Climate Change (IPCC) emission scenarios. *Global Biogeochemical Cycles*, **15**, 891–908.
- Kasischke ES, Turetsky MR (2006) Recent changes in the fire regime across the North American boreal region-Spatial and temporal patterns of burning across Canada and Alaska (vol 33, art no L09703, 2006). *Geophysical Research Letters*, **33**, doi: 10.1029/2006GL025677.
- Kurz WA, Dymond CC, Stinson G *et al.* (2008) Mountain pine beetle and forest carbon feedback to climate change. *Nature*, **452**, 987–990.
- Law BE, Falge E, Gu L *et al.* (2002) Environmental controls over carbon dioxide and water vapor exchange of terrestrial vegetation. *Agricultural and Forest Meteorology*, **113**, 97–120.
- Liu HP, Randerson JT (2008) Interannual variability of surface energy exchange depends on stand age in a boreal forest fire chronosequence. *Journal of Geophysical Research-Biogeosciences*, **113**, doi: 10.1029/2007JG000483.
- Liu HP, Randerson JT, Lindfors J, Chapin FS (2005) Changes in the surface energy budget after fire in boreal ecosystems of interior Alaska: an annual perspective. *Journal of Geophysical Research-Atmospheres*, **110**, doi: 10.1029/2004JD005158.

- Luyseart S, Schulze ED, Boerner A *et al.* (2008) Old-growth forests as global carbon sinks. *Nature*, **455**, 213–215.
- Lyons EA, Jin YF, Randerson JT (2008) Changes in surface albedo after fire in boreal forest ecosystems of interior Alaska assessed using MODIS satellite observations. *Journal of Geophysical Research-Biogeosciences*, **113**, doi: 10.1029/2007JG000606.
- Manies KL, Harden JW, Bond-Lamberty BP, O'Neill KP (2005) Woody debris along an upland chronosequence in boreal Manitoba and its impact on long-term carbon storage. *Canadian Journal of Forest Research-Revue Canadienne De Recherche Forestiere*, **35**, 472–482.
- Mcfadden JD, Ragotzki Ra (1967) Climatological significance of albedo in central Canada. *Journal of Geophysical Research*, **72**, 1135–1143.
- Mcmillan AMS, Goulden ML (2008) Age-dependent variation in the biophysical properties of boreal forests. *Global Biogeochemical Cycles*, **22**, doi: 10.1029/2007GB003038.
- Mitchell RG, Preisler HK (1998) Fall rate of lodgepole pine killed by the mountain pine beetle in central Oregon. *Western Journal of Applied Forestry (USA)*, **13**, 23–26.
- Myhre G, Highwood EJ, Shine KP, Stordal F (1998) New estimates of radiative forcing due to well mixed greenhouse gases. *Geophysical Research Letters*, **25**, 2715–2718.
- Pasch RJ, Blake ES, Cobb HD III, Roberts DP (2006) Tropical Cyclone Report Hurricane Wilma 15-25 October 2005. National Weather Service. National Hurricane Center. Tropical Prediction Center. Available at: http://www.nhc.noaa.gov/pdf/TCR-AL252005_Wilma.pdf (accessed 21 October 2011).
- Pfeifer EM, Hicke JA, Meddens AJH (2011) Observations and modeling of above-ground tree carbon stocks and fluxes following a bark beetle outbreak in the western United States. *Global Change Biology*, **17**, 339–350.
- Oak Ridge National Laboratory Distributed Active Archive Center (ORNL DAAC) (2011) MODIS subsetting land products, Collection 5. ORNL DAAC, Oak Ridge, TN, USA. Available at: <http://daac.ornl.gov/MODIS/modis.html> (accessed 3 June 2011).
- Raffa KF, Aukema BH, Bentz BJ, Carroll AL, Hicke JA, Turner MG, Romme WH (2008) Cross-scale drivers of natural disturbances prone to anthropogenic amplification: the dynamics of bark beetle eruptions. *BioScience*, **58**, 501–517.
- Randerson JT, Liu H, Flanner MG *et al.* (2006) The impact of boreal forest fire on climate warming. *Science*, **314**, 1130–1132.
- Roman MO, Schaaf CB, Woodcock CE *et al.* (2009) The MODIS (Collection V005) BRDF/albedo product: assessment of spatial representativeness over forested landscapes. *Remote Sensing of Environment*, **113**, 2476–2498.
- Romero LM, Smith TJ, Fourqurean JW (2005) Changes in mass and nutrient content of wood during decomposition in a south Florida mangrove forest. *Journal of Ecology*, **93**, 618–631.
- Rotenberg E, Yakir D (2010) Contribution of semi-arid forests to the climate system. *Science*, **327**, 451–454.
- Running SW (2008) Ecosystem disturbance, carbon, and climate. *Science*, **321**, 652–653.
- Russell RE, Saab VA, Dudley JG, Rotella JJ (2006) Snag longevity in relation to wildfire and postfire salvage logging. *Forest Ecology and Management*, **232**, 179–187.
- Safranyik L, Carroll AL, Wilson B (2006) The biology and epidemiology of the mountain pine beetle in lodgepole pine forests. In: *The Mountain Pine Beetle: A Synthesis of Biology, Management and Impacts on Lodgepole Pine*, pp. 3–66. Natural Resources Canada. Canadian Forest Service, Pacific Forestry Centre, Victoria, BC, Government of Canada.
- Schaaf CB, Gao F, Strahler AH *et al.* (2002) First operational BRDF, albedo nadir reflectance products from MODIS. *Remote Sensing of Environment*, **83**, 135–148.
- Schulze E, Heimann H (1998) Carbon and water exchange of terrestrial systems. In: *Asian Change in the Context of Global Climate Change: Impact of Natural and Anthropogenic Changes in Asia on Global Biogeochemistry*. (eds Galloway JN, Melillo JM), pp. 145–161. Cambridge University Press, New York.
- Schwind B (2008) Monitoring Trends in Burn Severity: Report on the Pacific Northwest and Pacific Southwest Fires – 1984 to 2005. Available at: <http://www.mtbs.gov/> (accessed 24 June 2010).
- Shell KM, Kiehl JT, Shields CA (2008) Using the radiative kernel technique to calculate climate feedbacks in NCAR's Community Atmospheric Model. *Journal of Climate*, **21**, 2269–2282.
- Smith T, Anderson G, Balentine K, Tiling G, Ward G, Whelan K (2009) Cumulative impacts of hurricanes on Florida mangrove ecosystems: sediment deposition, storm surges and vegetation. *Wetlands*, **29**, 24–34.
- Soden BJ, Held IM, Colman R, Shell KM, Kiehl JT, Shields CA (2008) Quantifying climate feedbacks using radiative kernels. *Journal of Climate*, **21**, 3504–3520.
- Stocks BJ, Mason JA, Todd JB *et al.* (2002) Large forest fires in Canada, 1959–1997. *Journal of Geophysical Research*, **107**, 8149, doi: 10.1029/2001JD000484.
- Wang K, Liang S, Schaaf CL, Strahler AH (2010) Evaluation of Moderate Resolution Imaging Spectroradiometer land surface visible and shortwave albedo products at FLUXNET sites. *Journal of Geophysical Research (Atmospheres)*, **115**, 17107, doi: 10.1029/2009JD013101.
- Waring RH, Pitman GB (1985) Modifying lodgepole pine stands to change susceptibility to mountain pine-beetle attack. *Ecology*, **66**, 889–897.
- Westerling AL, Hidalgo HG, Cayan DR, Swetnam TW (2006) Warming and earlier spring increases western U.S. forest wildfire activity. *Science*, **313**, 940–943.
- Westfall J, Ebata T (2009) *Summary of Forest Health Conditions in British Columbia-2008*. British Columbia Ministry of Forests, Forest Practices Branch, Victoria, BC, Canada.
- Xiao XM, Zhang QY, Braswell B *et al.* (2004) Modeling gross primary production of temperate deciduous broadleaf forest using satellite images and climate data. *Remote Sensing of Environment*, **91**, 256–270.
- Zeng HC, Chambers JQ, Negron-Juarez RI, Hurtt GC, Baker DB, Powell MD (2009) Impacts of tropical cyclones on US forest tree mortality and carbon flux from 1851 to 2000. *Proceedings of the National Academy of Sciences of the United States of America*, **106**, 7888–7892.

Supporting Information

Additional Supporting Information may be found in the online version of this article:

Appendix S1. Model fits (functions with fitted coefficients and fitting statistics) for the seasonal and annual time series of albedo following boreal fire shown in Figure 7.

Please note: Wiley-Blackwell are not responsible for the content or functionality of any supporting materials supplied by the authors. Any queries (other than missing material) should be directed to the corresponding author for the article.